

## MAST magnetic diagnostics

T. Edlington, R. Martin, and T. Pinfold

Citation: *Rev. Sci. Instrum.* **72**, 421 (2001); doi: 10.1063/1.1309009

View online: <http://dx.doi.org/10.1063/1.1309009>

View Table of Contents: <http://rsi.aip.org/resource/1/RSINAK/v72/i1>

Published by the American Institute of Physics.

---

### Related Articles

Generating electron cyclotron resonance plasma using distributed scheme  
*Appl. Phys. Lett.* **101**, 062414 (2012)

Dissociative electron attachment to C<sub>2</sub>F<sub>5</sub> radicals  
*J. Chem. Phys.* **137**, 054310 (2012)

Hanle effect as candidate for measuring magnetic fields in laboratory plasmas  
*Rev. Sci. Instrum.* **83**, 10D528 (2012)

Improved analysis techniques for cylindrical and spherical double probes  
*Rev. Sci. Instrum.* **83**, 073506 (2012)

Dielectric covered hairpin probe for its application in reactive plasmas  
*Appl. Phys. Lett.* **101**, 042105 (2012)

---

### Additional information on Rev. Sci. Instrum.

Journal Homepage: <http://rsi.aip.org>

Journal Information: [http://rsi.aip.org/about/about\\_the\\_journal](http://rsi.aip.org/about/about_the_journal)

Top downloads: [http://rsi.aip.org/features/most\\_downloaded](http://rsi.aip.org/features/most_downloaded)

Information for Authors: <http://rsi.aip.org/authors>

### ADVERTISEMENT

The advertisement features the AIP Advances logo at the top, which includes the text "AIP Advances" with orange dots above it. Below the logo is a green banner containing the text "Special Topic Section: PHYSICS OF CANCER" in white, bold letters. At the bottom of the banner, the question "Why cancer? Why physics?" is displayed in white, and a blue button on the right says "View Articles Now". The background of the ad is a green and yellow abstract design.

# MAST magnetic diagnostics

T. Edlington,<sup>a)</sup> R. Martin, and T. Pinfold

*EURATOM/UKAEA Fusion Association, Culham Science Centre, Abingdon, Oxon. OX14 3DB, United Kingdom*

(Presented on 19 June 2000)

The mega-ampere spherical tokamak (MAST) experiment is a new, large, low aspect ratio device ( $R=0.7\text{--}0.8\text{ m}$ ,  $a=0.5\text{--}0.65\text{ m}$ , maximum  $B_T \sim 0.63\text{ T}$  at  $R=0.7\text{ m}$ ) operating its first experimental physics campaign. Designed to study a wide variety of plasma shapes with up to 2 MA of plasma current with an aspect ratio down to 1.3, the poloidal field (PF) coils used for plasma formation, equilibrium and shaping are inside the main vacuum vessel. For plasma control and to investigate a wide range of plasma phenomena, an extensive set of magnetic diagnostics have been installed inside the vacuum vessel. More than 600 vacuum compatible, bakeable diagnostic coils are configured in a number of discrete arrays close to the plasma edge with about half the coils installed behind the graphite armour tiles covering the center column. The coil arrays measure the toroidal and poloidal variation in the equilibrium field and its high frequency fluctuating components. Internal coils also measure currents in the PF coils, plasma current, stored energy and induced currents in the mechanical support structures of the coils and graphite armour tiles. The latter measurements are particularly important when halo currents are induced following a plasma termination, for example, when the plasma becomes vertically unstable. The article describes the MAST magnetic diagnostic coil set and their calibration. The way in which coil signals are used to control the plasma equilibrium is described and data from the first MAST experimental campaign presented. These coil data are used as input to the code EFIT [L. Lao *et al.*, Nucl. Fusion **25**, 1611 (1985)], for measurement of halo currents in the vacuum vessel structure and for measurements of the structure of magnetic field fluctuations near the plasma edge. © 2001 American Institute of Physics. [DOI: 10.1063/1.1309009]

## INTRODUCTION

Accurate measurements of currents and magnetic fluxes in tokamak experiments are a fundamental diagnostic requirement for determining the evolution of plasma equilibrium, plasma stability and confinement. Increasingly important, for large devices, are measurements, which allow the plant to operate within safe boundaries, protecting the structure from forces generated by halo currents. The mega-ampere spherical tokamak (MAST) experiment is equipped with a comprehensive set of magnetic diagnostics, which aim to satisfy this requirement.

The MAST vacuum vessel<sup>1</sup> is a 4.4-m-high stainless steel cylinder with two flat 4-m-diam end plates. A vertical Inconel center tube separates the center rod, which generates the toroidal field, and the center solenoid from the vacuum. The remaining five pairs of poloidal field coils are contained inside the vacuum vessel in stainless steel cans supported from the vacuum vessel wall. The coil cans are electrically connected to the vessel both via the mechanical support structure and by the vacuum bellows connection of feeder bars at vessel ports. The vacuum vessel is bakable to 200 °C requiring all internal magnetic diagnostics to be compatible with continuous operation at this temperature.

Single null and double null operation with an open diverter structure limits the coverage of the poloidal cross sec-

tion by diagnostic coils. The gap in reconstructing the poloidal field structure is partly filled by including coils and loops behind the armour tile that protects the P2 divertor coil from the inner and outer strike points. Halo currents in the center tube and the poloidal field (PF) support structure could generate bending forces beyond the design limits of the experiment. Operation at the maximum plasma current of 2 MA relies on measurements during lower plasma current operation to confirm design assumptions, about the amplitude and distribution of these currents.

## EXPERIMENTAL ARRANGEMENT

Lowest possible aspect ratio with a high center rod current and reasonable solenoid flux swing leaves little space available for magnetic diagnostics in the center column design. On the vacuum side of the Inconel tube 18 mm are allocated between the tube and the plasma for graphite tiles and their support. The magnetic diagnostics are designed as an integral part of the armor tile assembly as shown schematically in Fig. 1.

Each graphite tile is 16 mm thick and 11 rows, each of three, 305 mm high tiles protect the center column. The tiles are supported by a clamped ring at the bottom of the center tube and are spaced 2 mm away from the tube by spring loaded feet. Each row of tiles has a 5-mm-deep horizontal groove at the mid-plane to accommodate magnetic diagnostic coils. At 60° intervals there are also 5-mm-deep vertical

<sup>a)</sup>Electronic mail: trevor.edlington@ukaea.org.uk

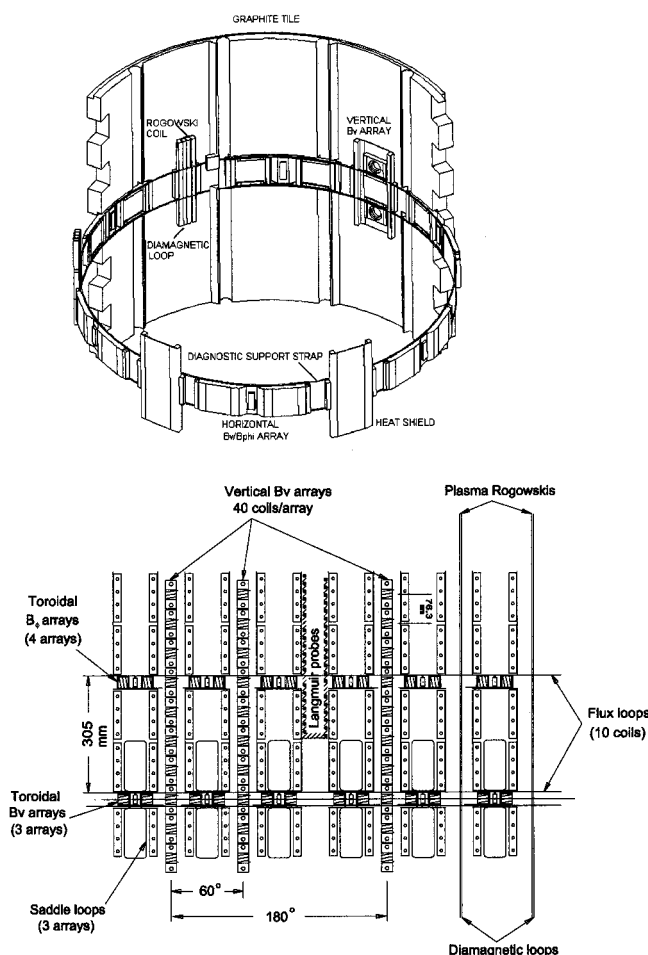


FIG. 1. Schematic view of support and layout of center column diagnostic coils and loops. Only a short section of the center column is shown for clarity.

grooves. Eleven Inconel straps, aligned with horizontal grooves in the graphite, support magnetic diagnostics. Toroidal arrays of coils are fastened to these straps in sub-assemblies of pairs of coils. In some cases these sub-assemblies also include a local saddle loop. In each horizontal groove a full toroidal flux loop is clipped to the edge of the Inconel strap. Larger sub-assemblies containing three vertical arrays, each of  $B_v$  coils, and the two plasma current and diamagnetic loop assemblies are supported between the straps at toroidal locations aligned to the positions of the vertical grooves in the graphite. The sixth groove is used for Langmuir probes, which protrude slightly through holes in the graphite tile. All discrete coils are wound on a machined ceramic former using 0.3-mm-diam armored Poly-Thermalese 2000 wire. Flux loops and saddle coils use a single turn of the same wire with high temperature PTFE sleeve inside thin walled stainless steel tubing. At toroidal locations radially aligned with the three center column vertical arrays of  $B_v$  coils are three outer arrays of pick up coils. Each array has 19 sub-assemblies, each containing, on a common ceramic insulator, a pair of orthogonal coils with the same center. The assembly is mounted on a stainless steel rail supported from the outer cylinder of the vacuum vessel. Insulating breaks are used to prevent induced currents in the

support structure and each pair of coils has a thin graphite cap to prevent plasma interaction with the coils. Additional flux measurements are made using loops attached to the PF coil cases and to the stainless steel P2 graphite support plate. Large area saddle loops are also attached to the inside surface of the cylindrical vacuum vessel. Three rectangular loops, at different heights are attached around diagnostic ports at each of the 12 sectors of the vacuum vessel. At the top and bottom of the plasma, further discrete coils are built into the P2 divertor coil protection plate. Sub-assemblies containing four coils are mounted between an annular stainless steel plate and the graphite armor tiles. Each radial array contains eight coils which measure the radial component of the field at the same plasma poloidal cross section as the center column vertical  $B_v$  and outer  $B_v/B_\phi$  coils. The relative positions of the discrete coil arrays at a poloidal cross section are shown in Fig. 2. Signals from coils separated toroidally by  $180^\circ$  are summed to remove  $n=1$  components before integration and digitization.

The construction of the Rogowski coils and diamagnetic loop coils is summarized in Fig. 3. Three types of Rogowski coil are used on the MAST experiment. For the feeder bar currents outside the vacuum vessel a commercially available high sensitivity Rogowski coil is used. Inside the vacuum vessel, because of the space and vacuum restrictions, custom solutions are required. Fifty-two full Rogowski coils are installed inside the vessel. Two types of winding are used for all the coils as shown in Figs. 3(a) and 3(b). The plasma current, center rod and halo current Rogowski coils are all of the type shown in Fig. 3(a). Here a single layer of turns is used with a coaxial return conductor. All PF case Rogowski coils are wound as shown in Fig. 3(b) with a second layer of turns to increase the sensitivity. In this case no return conductor is necessary to cancel the toroidal field (TF) flux. In both cases the coil is wound on a thin walled stainless steel tube insulated with high temperature PTFE heat-shrink which is also used to cover the coil. The plasma current and halo current Rogowski coils are then contained in a second stainless steel tube while the PF Rogowski coils fit in a machined groove in a frame around the PF coil case covered on any plasma facing view with graphite. Any induced currents in the PF coil cases are measured by the internal PF Rogowski coils and can be determined separately by subtracting the feeder bar current. The induced current in the center Inconel tube can also be determined by subtracting the TF feeder bar current from the internal center rod Rogowski coil signal.

The plasma current Rogowski is made in four long, straight sections. Two 2 m sections are supported from the end plates of the vacuum vessel, with two 4 m vertical sections supported from the outer cylinder and the center Inconel tube. Signals from the four sections are brought out of the vacuum vessel and digitized separately. The plasma current is reconstructed both by real time analog electronics and by software after the shot by subtracting all PF coil case Rogowski signals. Allowance has also to be made for induced currents in other conducting parts of the internal vacuum vessel structure.

The diamagnetic loop is also manufactured in four long

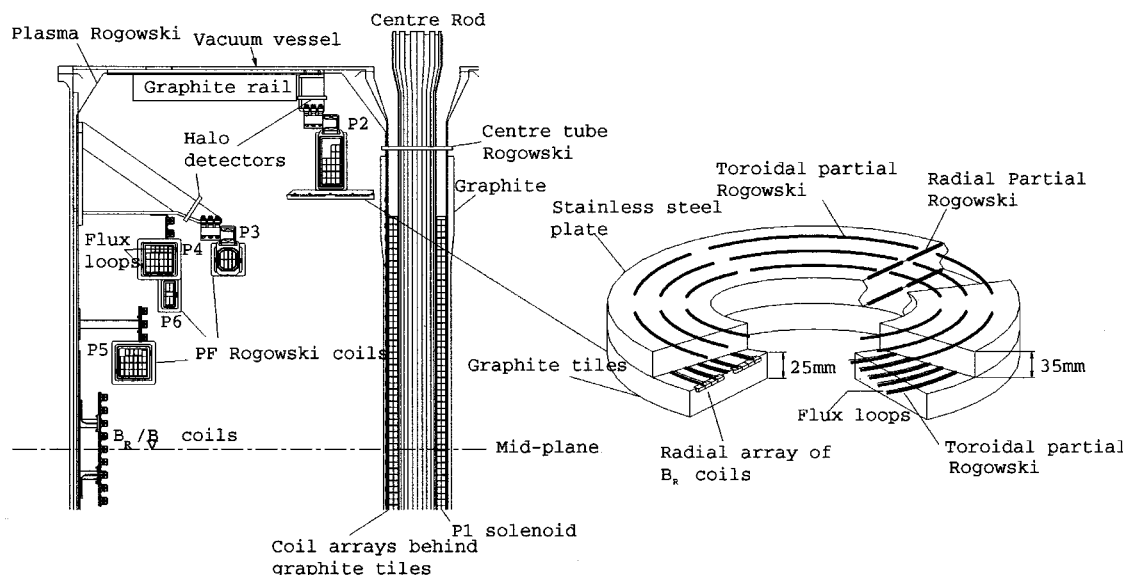


FIG. 2. Cross section of part of the MAST vacuum vessel showing the location of some of the internal magnetic diagnostic coils. The exploded view of the P2 coil protection plate shows schematically how diagnostic coils have been built into the graphite support structure.

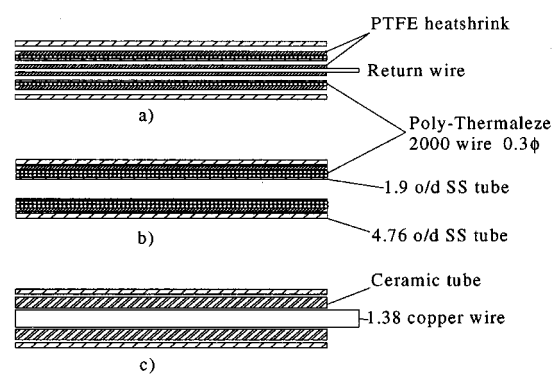
sections. The arrangement is shown in Fig. 3(c). In this case however an in-line joint has been made inside the vacuum vessel between the sections and only a single signal is brought out at the vacuum feedthrough. Ceramic beads are used at the bends to insulate the wire in the center of the tube. TF compensating signals are generated from a specially wound Rogowski on the TF feeder bar and from a dedicated multi-turn coil measuring the TF field inside the vacuum vessel with approximately the same sensitivity as the diamagnetic loop.

Halo currents are measured by detectors around each of the six support legs of P2 and P3 PF coils (see Fig. 2). The current feeds for these coils come through bellows connections at diagnostic ports and this potential current path is also monitored (not shown in the diagram). Center column Rogowski coils are used to determine the total halo current in the Inconel center tube and its distribution can be deduced from four toroidal arrays of  $B_\phi$  coils at different heights on the center column. During terminations where the plasma moves vertically, currents are induced in the P2 armor tile support plates. Arrays of partial Rogowski coils have been installed in both sides of the plate as shown in Fig. 2 to determine the distribution of this current.

## CALIBRATION

Bench-top calibration of the single element internal and external Rogowski coils against a previously calibrated reference was done prior to installation. The average calibration factors and the standard deviation for each group of coils are shown in Fig. 3. The accuracy of each individual calibration was estimated to be 0.1%. The plasma current Rogowski was calibrated *in situ* with respect to the PF Rogowski using current pulses in individual PF coils, with data taken at the end of a long flat-top pulse to allow induced currents to decay. The variation in PF Rogowski coil measurements for individual coils was between 0.1% and 0.45%. Data from eight vacuum shots with current pulses in individual PF coils

were used in a matrix solver to determine the equivalent calibration factors for the four individual segments of the plasma current Rogowski. Further correction to the plasma current signal is necessary to remove the contribution from toroidal currents induced in the P2 armor tiles and its support plate. This current is estimated from the innermost and outermost P2 plate flux loop signals using vacuum shots with the solenoid and P3 coil energised from capacitor banks to calculate the two coefficients. After correction the net current measured by the plasma current on any vacuum shot is  $<\pm 2$  kA with a standard deviation on these net signals of  $\pm 1$  kA. Imperfections in the Rogowski coils leads to pick-up from all the PF currents which has to be subtracted. The total effect of these pick-up terms after subtraction is estimated to be



Coil	Sensitivity Vs/A	$\sigma$
PF Rogowski	3.75E-06	4.13E-08
Halo Rogowski	2.05E-08	6.02E-10
External Rogowski	5.14E-08	1.43E-09

FIG. 3. Construction of Rogowski coils (a), (b) and diamagnetic loop (c). Dimensions shown are all mm. The table shows the mean Rogowski coil calibration values and the standard deviation  $\sigma$  of the calibration factors for each group of coils.

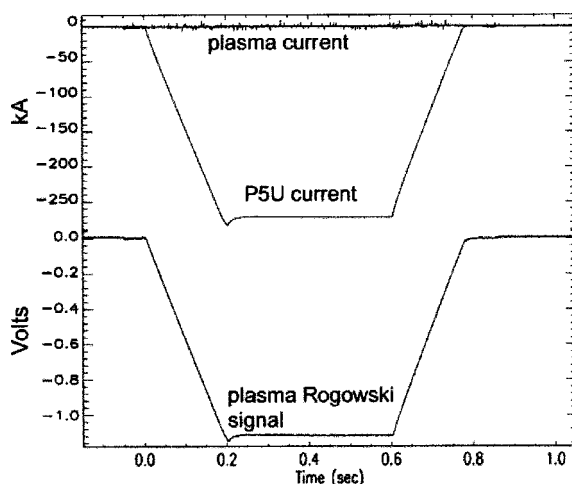


FIG. 4. Residual plasma current measurement for a vacuum shot using P5U only.

<0.05%. Figure 4 shows a vacuum shot with current in the upper P5 coil only. The waveforms show the P5 current, the sum of the four Plasma Rogowski coil segments and the residual signal after subtraction of the P5 current and compensation for induced currents and other pick up terms. Fast spikes on the signal, which are slightly larger than the  $\pm 1$  kA calibration accuracy are caused by the converter power supplies used for the PF circuits.

## RESULTS

The MAST magnetic diagnostic coil set has been successfully commissioned. The first period of MAST operation has been committed to developing plasma generation scenarios that achieve stable, large volume, low aspect ratio plasmas suitable for neutral beam injection (NBI) and electron cyclotron resonance heating (ECRH) experiments. Early emphasis on vacuum vessel conditioning techniques has allowed access to H modes during NBI experiments. So far, low aspect ratio tokamak plasmas have been generated with plasma current up to 1.1 MA. The magnetic diagnostics have been crucially important in establishing stable and safe operation at this level. Figure 5 shows typical waveforms from a high current shot. The plasma current traces from post-shot reconstruction and from real-time analog electronics are both shown. The analog signal is less accurate at present because the P2 plate induced currents are not included. The loop voltage signal comes from one of the two mid-plane center column flux loops. During the current rise phase a number of internal magnetic reconnection events (IREs) can occur which do not lead to plasma termination. The IRE's and other MHD phenomena are observed on many of the discrete coil arrays. Coil array signals at one poloidal cross section and a complete toroidal array at the plasma mid-plane are digitized separately at a higher speed (up to 1 MHz) allowing the spatial structure of the modes to be studied. Fast data from a mid-plane center column Mirnov coil is included in Fig. 5 and shows, apart from large effects linked to the IREs a more continuous level of high frequency fluctuations which reduce in amplitude as the peak plasma current is reached.

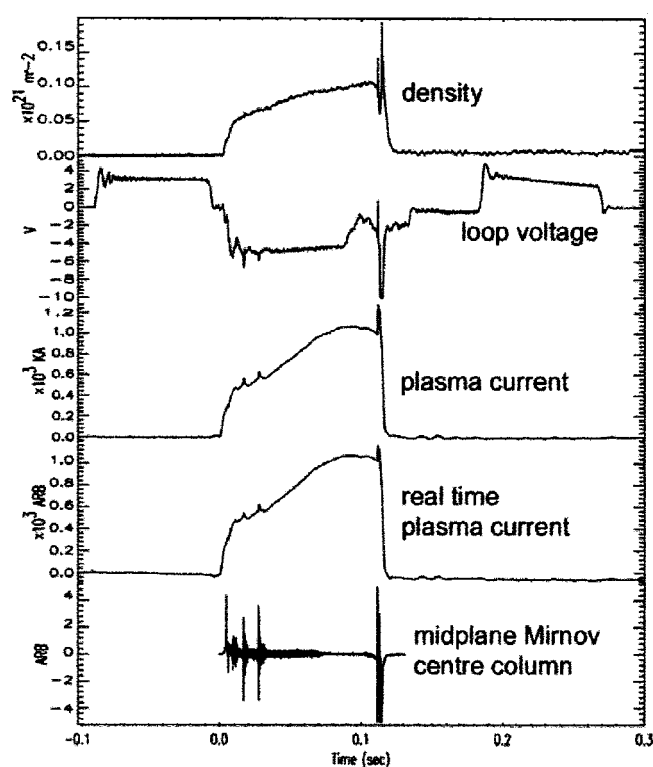


FIG. 5. Waveforms for MAST Shot 2482 ( $I_p \sim 1$  MA) showing line integral density, loop voltage, two plasma current signals and a non-integrated signal from a mid-plane  $B_v$  coil. The upper plasma current trace is reconstructed by analysis after the shot. The lower trace is a real time reconstruction from analog electronics.

During this period of initial MAST operation, the relatively short center solenoid has been used without including the eight turn compensating winding included in the P2 coil pack. The consequence of this is that most shots end with an IRE induced vertical displacement event (VDE) as the stray field from the solenoid becomes destabilizing when the solenoid current reverses. The resulting halo currents for a downwards VDE in a relatively low plasma current shot are shown in Fig. 6. Several distinct types of VDE termination have been identified and their characteristics tabulated. A large database of halo current behavior has now been

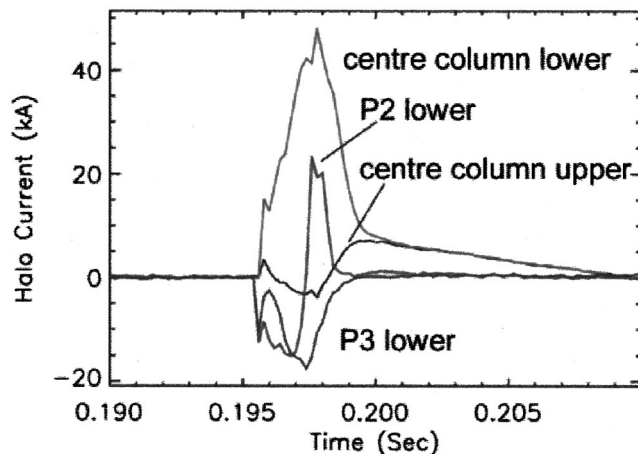


FIG. 6. Total halo currents in P2/P3 supports and center column for shot 2223 ( $I_p \sim 390$  kA) which ends with a downward VDE.

accumulated<sup>2</sup> showing that, for MAST, high halo current fractions (up to 50%) occur only at low plasma current where the plasma is small and relatively high aspect ratio. For large volume, low aspect ratio plasmas with high plasma current (up to 1 MA), the halo current fraction measured to date is always lower than 25%. Toroidal asymmetries have only been observed when the halo current fraction is small or for a short time when the current first enters the center column when a clear  $n=1$  structure is sometimes observed. These initial measurements of halo currents suggest that, for opera-

tion of MAST at 2 MA, the forces generated by halo currents will be within the design limits of the experiment.

#### ACKNOWLEDGMENTS

This work is jointly funded by the UK Dept. of Trade and Industry and by Euratom.

<sup>1</sup>A. Darke *et al.*, Proceedings of the 16th IEEE/NPSS Symposium on Fusion Engineering, Illinois, 1995, p. 1456.

<sup>2</sup>R. Martin *et al.*, 27th European Physical Society Conference on Controlled Fusion and Plasma Physics, Budapest, Hungary, 2000.